Appl. Phys. B 55, 132–137 (1992)

Applied Physics B Photophysics and Laser Chemistry

Bifurcation Structures into Chaos of Delay-Differential Equations for a Passive Optical Ring Resonator

Ch. Häger* **and F. Kaiser**

Technical University Darmstadt, Institute of Applied Physics – Nonlinear Dynamics, Hochschulstrasse 4a, W-6100 Darmstadt, Fed. Rep. Germany

Received 31 January 1992/Accepted 6 April 1992

Abstract. The delay-differential equation system describing the passive optical ring cavity is investigated. A survey of different bifurcation scenarios into chaos of the solutions on one branch and specific transitions between different branches of the multistable system are discussed. Precipitation via a heteroclinic cycle and crisis induced intermittency are found.

PACS: 42.65.Pc

Nonlinear optics exhibits a variety of temporal and spatio-temporal structures. In the moment there is much interest in transverse instabilities which involve a high number of degrees of freedom. Some years ago there have been some publications concerning optical delay systems. Although systems with time delay require a highly complex mathematical analysis, detailed information is requested in order to understand a great number of real physical systems, e.g., class B laser. Since the understanding of these systems is far from being complete, we have performed numerical investigations with the delay-differential equations of Ikeda [1].

These equations are infinite dimensional in time and describe an optical ring cavity. However, in most cases the equations are treated in a simplified version (Ikeda map). It was doubted whether the map describes the dynamics of the system in a sufficent manner [2] and in some later papers these doubts were confirmed [3–5]. For this reason we will treat the ring cavity in the original description of Ikeda and without any simplifications. The delay-differential equation system (ddeq) reads:

$$\frac{\partial \Phi(t)}{\partial t} = -[\Phi(t) + 1/2] - 2/\alpha L |E(t-\gamma\tau)|^2 \times \{\exp[2\alpha L \Phi(t)] - 1\}, \quad (1)$$

$$E(t) = \sqrt{T} E_i + RE(t-\gamma\tau)\exp[\alpha L \Phi(t)] \times \exp\{-i\alpha L \Delta\omega[\Phi(t) + 1/2] - i\delta\}. \quad (2)$$

The meaning of the variables and parameters is as follows: $E(t)$ is the complex, slowly varying envelope of the electric field at the inner boundary of the input mirror and $\Phi(t)$ is the atomic inversion averaged over the two-level medium with length L. The dimensionless time t is scaled on the longitudinal relaxation rate γ and the delay-parameter $\gamma\tau$ gives the time the light needs to travel once around the cavity. The parameter δ represents the empty-cavity detuning. Other parameters are the atomic detuning $\Delta\omega$, the amplitude of the input field outside the cavity E_i, the absorption α, and the susceptibility $\chi = \alpha\Delta\omega$. R and T are the reflectivity and transmittivity of the input and output mirrors respectively. For further details see [5, 6] and references cited therein.

In recent papers some aspects of the simulation of the delay-differential equation system were explained. In the first, an example for each of the different routes to chaos was given [6], in the second, one of the routes was investigated by using a Lyapunov analysis [7]. In the third paper the linear stability analysis of the equations was performed [5]. In this article we shall show a survey of the three different routes to chaos in the relevant $\delta - \gamma\tau$ space of parameters. In addition, we will examine some typical processes of fundamental interest. These include precipitation and intermittent transitions between different branches. Both phenomena might be relevant for switching processes in real optical devices. These extended investigations give us more details on the possible temporal structures and bifurcations in the ring cavity. This information is also highly requested when analysing the spatio-temporal structures in the system. At the moment it is not feasible to analyse a transverse system including time delay because of the infinite number of dimensions not only in space but also in time. For this reason only systems with either transverse coupling (see, e.g., [8]) or with time delay are treated. The information of the delay system and of the system with transverse coupling give help for an analysis of the complete system.

* Present address: Institut für physikalische und theoretische Chemie, J.W. Goethe-Universität, W-6000 Frankfurt/M 50, Fed. Rep. Germany

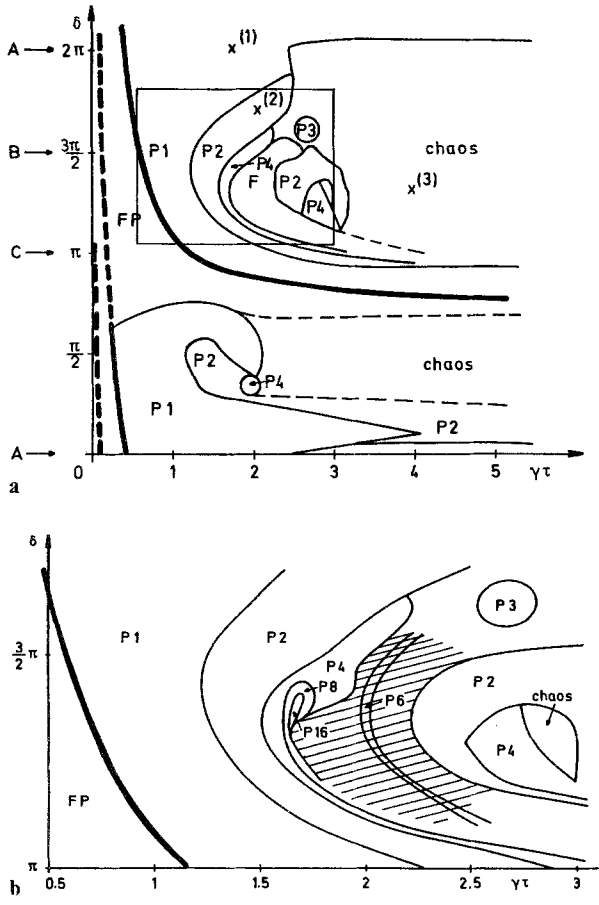

Fig. 1a, b. Bifurcation structures in the parameter space: **a** Cavity detuning δ vs delay-parameter $\gamma\tau$ at $E_i = 3$, $R = 0.95$, $\alpha L = 4$, $\chi L = 12\pi$; **b** Extended part of the parameter space δ vs $\gamma\tau$ (description see text)

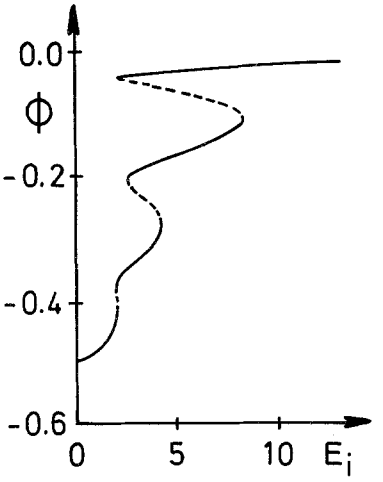

Fig. 2. Stationary solutions of the averaged inversion Φ vs the outside input amplitude E_i ($\delta = \frac{3}{2}\pi$, $\gamma\tau \to 0$)

1 Bifurcation Structures in Parameter Space

In [6] the authors presented three different routes to chaos for different values of the parameter δ with increasing parameter $\gamma\tau$: Intermittency route at $\delta = 0 \equiv \delta = 2\pi$, period-doubling route at $\delta = \pi$, and quasi-periodicity at $\delta = \frac{3}{2}\pi$. We are now interested in the question how these different routes turn into each other by continuous variation of δ. To this end, we computed a section through the parameter space, keeping all parameter constant except δ and $\gamma\tau$ ($E_i = 3$, $R = 0.95$, $\alpha L = 4$, $\chi L = 12\pi$). It should be stressed, that $\gamma\tau$ and δ are not independent from each other and therefore special setups are requested for a real experiment.

The result of our calculation can be seen in Fig. 1, where the empty-cavity detuning δ vs the delay-parameter $\gamma\tau$ is shown. The arrows in the left of the ordinate of Fig. 1a mark the three routes to chaos already mentioned. The letters A,B,C stand for the intermittency route, the quasi-periodicity and the period-doubling route respectively.

In Fig. 1a the reader recognizes a bold line beginning on the right hand side at $\gamma\tau \approx 5$, $\delta \approx 0.8\pi$. It is continued at $\gamma\tau \approx 0.3$, $\delta = 0$, leading to the top again and is continued a third time in the lower left. At this line the first Hopf bifurcation occurs when $\gamma\tau$ is increased. On the left of it (at small values of $\gamma\tau$) the attractor is a stable fixed point (marked by FP), on the right of it periodic, quasi-periodic and chaotic solutions exist. The figure shows the behaviour of the system on the lower branch but the dashed continuation of the bold line is the boundary of the first Hopf bifurcation on the upper branches because δ goes modulo 2π. In Fig. 2 the multistability curve shows three stable branches for $E_i = 3$. In the following we use the position of the branches relative to the inversion to classify them in *upper*, *middle*, and *lower branch*.

The periodic solutions on the lower branch are marked by P_i, (i indicates the periodicity). For the period-doubling route they were discriminated up to the P_{64}-solution for some values of the parameters. A sequence of period-doublings at $\delta = \pi$ is shown in [6].

The mode-locking region (F) lies in the upper part of the figure between the period-4 and the period-2 solution. At the left boundary of this region the system undergoes a second Hopf bifurcation. As explained in detail in [6] a new frequency ω_2 is generated, which is incommensurable to the first one, ω_1. In this reference for the case of $\delta = \frac{3}{2}\pi$, mode-locking of the two frequencies was found, beginning at a winding-number $\omega_2/\omega_1 = \frac{3}{2}$ and ending at $\omega_2/\omega_1 = \frac{3}{2}$. A modified devil's staircase (nonstandard Farey sequence) is found by applying the Farey tree construction. The explicit calculation of the winding numbers is given in [6]. The values of the frequencies have been identified by Fourier spectra of the time series. It should be stressed, that our definition of the winding number is arbitrary and the reversed definition (ω_1/ω_2) is suited as well.

Figure 1b shows a detail of Fig. 1a, demonstrating the occurrence of period-doubling and mode-locking in narrow neighboured regions of parameter space. For $\delta = \pi$ the period-doubling route can be followed up to period-4 in this diagram. At increasing values of δ, the branches between the periodic solutions shift to the left and the mode-locking region (hatched) occurs. In this region the widest resonance ($\omega_2/\omega_1 = \frac{5}{6}$, marked by P_6) is also shown. All other resonances are much smaller and cannot be resolved on this scale. It should be noted, that the period-doubling sequence is only interrupted by the mode-locking region, it continues in part again at higher values of $\gamma\tau$.

In the mode-locking region specific period-doubling bifurcations occur, e.g., the transition $\omega_2/\omega_1 = \frac{5}{6}$ to a $\omega_2/\omega_1 =$

$\frac{10}{12}$. There are quasi-periodic and even chaotic solutions between the mode-locked tongues. This indicates, that there is probably no complete Farey sequence for any parameter set. For the chosen values of parameters the regions with irrational winding-numbers do not form a Cantor set.

2 Coexistence and Jumps Between the Stable Branches

The property of multistability of the system was explained in detail in [5] (see Figs. 1 and 2 of this reference). Here we investigate specific dynamical solutions of the different branches: The coexistence of periodic and chaotic solutions, crisis induced intermittency between two branches and the process of precipitation from one branch to another one.

Out of a variety of solutions we discuss three cases in the parameter space. Each of them is found in large regions of the parameter space. In Fig. 1a the three points are indicated by an X and numbered in the following sequence:

(1) Coexistence of periodic solutions ($\delta = 0$, $\gamma\tau = 1.75$);

(2) Precipitation from upper to lower branch ($\delta = 1.7\pi$, $\gamma\tau = 2.15$);

(3) Intermittent jumps between middle and lower branch ($\delta = 1.3\pi$, $\gamma\tau \geq 3.1$).

We shall give explanations of the processes in the next three Sects.

2.1 Coexistence of Periodic Solutions

By a variation of the initial conditions it is possible to select the branch on which the system starts its trajectory. Two coexistent periodic solutions on the upper and the lower branch were found in this way. Figure 3 shows the positions of the attractors relative to each other in three-dimensional physical phase space spanned by the real and imaginary part of the transmitted electrical field and the atomic inversion. In the parameter region under consideration there exist only two stable oscillating branches. The different limit-cycles are labeled with $(L1)$ and $(L2)$ in Fig. 3.

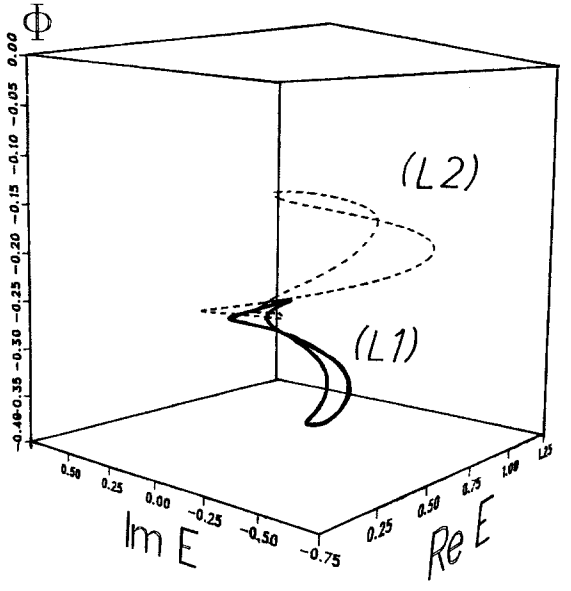

Fig. 3. Two coexistent solutions on lower $(L1)$ and upper $(L2)$ branch at $\delta = 2\pi$, $\gamma\tau = 1.75$ in the three-dimensional physical phase space spanned by the variables $\mathrm{Re}\{E\}$, $\mathrm{Im}\{E\}$, and Φ

Similar to the scenario described in Sect. 1 for the lower branch, the first Hopf bifurcation on the upper branch takes place at lower values of the parameter $\gamma\tau$ compared with the Hopf bifurcation on the lower branch. In Fig. 4 details of the two attractors are displayed. A detailed examination of the time-series (Fig. 4c) and the power spectra (Fig. 4d) shows that the solution on the upper branch oxcillates about three times as fast as the solution on the lower branch. The ratio of the frequencies is $\omega_{(L1)} : \omega_{(L2)} \approx 0.341\ldots$. The Hopf bifurcations on the different branches generate limit-cycles with different frequencies.

Figure 3 shows that the two attractors lie very close together. The separating saddleorbit between the two branches can be crossed at other values of the parameters. This case will be treated in the subsequent Sects.

2.2 Precipitation Between two Branches

We will consider now the case of unstable solutions on one or two branches and one stable solution on the third branch.

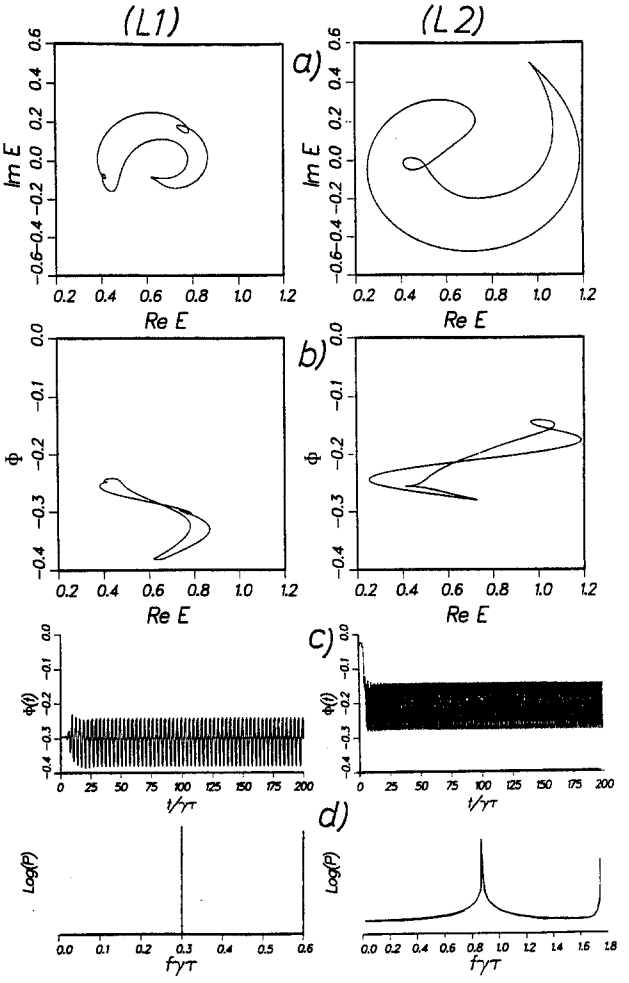

Fig. 4a–d. Both coexistent solutions on lower $(L1)$ and upper $(L2)$ branch at $\delta = 2\pi$, $\gamma\tau = 1.75$. **a** Phase space: $\mathrm{Im}\{E\}$ vs $\mathrm{Re}\{E\}$; **b** Phase space: Φ vs $\mathrm{Re}\{E\}$; **c** Time dependence of the inversion Φ; **d** Power spectra of the solutions

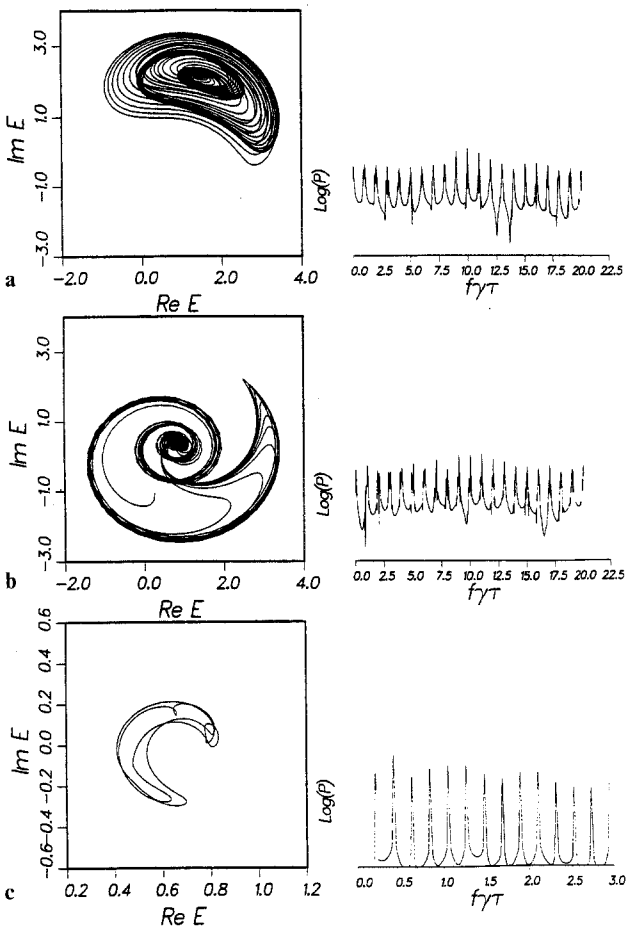

Fig. 5a–c. Sequence of phase space projections in the plane of the complex electrical field $\mathrm{Im}\{E\}$ vs $\mathrm{Re}\{E\}$ and power spectra at $\delta = 1.7\pi$, $\gamma\tau = 2.15$ on the three branches with different transient times. **a** Saddlefocus on the upper branch ($t/\gamma\tau \approx 100$ to 110); **b** Saddlefocus on the middle branch ($t/\gamma\tau \approx 220$ to 230); **c** Stable solution on lower branch

Such a transition between the branches was called precipitation [6, 9].

For example at $\delta = 1.7\pi$, $\gamma\tau = 2.15$, the lower branch shows a stable period-2 solution. By choosing the initial conditions to be on the upper branch, one gets a quasi-periodic saddlefocus at first.

The quasi-periodicity and the saddle property of the solution can be seen in Fig. 5a; the trajectory spirals inwards and outwards the unstable stationary point and the region visited by the trajectory is expanding slowly in phase space. The power spectrum shows two incommensurable frequencies with ratio $\omega_1/\omega_2 \approx 1/11$. A local stability analysis has yet to be performed to prove the conjectured saddlefocus behaviour.

The solution is not stable for long times: After about 300 cavity transit times the trajectory comes near to the saddle which seperates the two branches and precipitates to the middle branch (see Fig. 6c). This branch again is a quasi-periodic saddlefocus but only with an one-dimensional stable manifold (see Fig. 5b). Both branches are connected by a heteroclinic orbit with an one-dimensional manifold (the thin black line connecting both saddles in the figure) while falling from the upper to the middle branch and by a heteroclinic

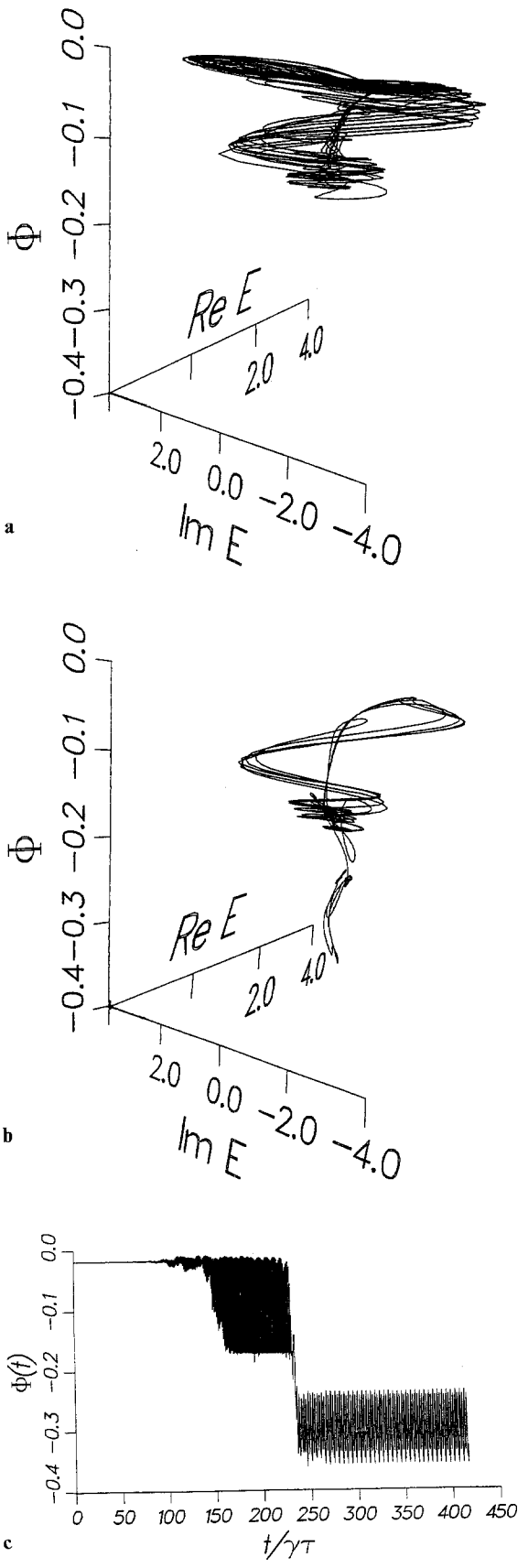

Fig. 6a-c. Heteroclinic orbit at $\delta = 1.7\pi$, $\gamma\tau = 2.15$. **a** and **b** projection of the trajectory in three-dimensional physical phase space, spanned by the complex electrical field E and the inversion Φ: **a** Time $t/\gamma\tau$ runs from 150 to 160; **b** $t/\gamma\tau \approx 225$ to 238; **c** Time series with initial conditions on upper branch for $t/\gamma\tau = 0$ to 400

orbit with a two-dimensional manifold while passing from the middle to the upper branch. The terminology is explained in [10].

After overcoming the saddle between the middle and the lower branch after some transients the system shows the period-2 solution of the lower branch (Fig. 5c).

In three dimensions, the behaviour of the trajectory between the upper and the middle branch can be described by the formation of a heteroclinic cycle which transforms into a homoclinic orbit on the middle branch. Both are only transients to the stable solution P_2 on the lower branch. A presentation of the whole precipitation process from upper to middle and then to lower branch is given in Fig. 6. Here, the one-dimensional heteroclinic connection between the upper and the middle branch can be seen as a sharp line in comparison with the two dimensional connection from the middle to the lower branch, which spirals around it. This phenomenon of precipitation is found also in completely different regions of the parameter space.

It turns out that precipitation is linked with the occurence of long transients. Presumably, the trajectory is wandering around in certain regions of phase space until it finds a path where it can cross the regular or fractal boundary seperating the different solutions.

An experimental evidence for the appearance of heteroclinic cycles in nonlinear optical systems such as ours, i.e., systems involving both eletric field and inversion as dynamical variables, gives [11]. There, a laser with feedback is considered. In analogy to the Ikeda ddeqs (1, 2), the equations describing this setup have been derived from the Maxwell-Bloch equations, too.

2.3 *Intermittent Jumps Between two Branches*

Also this type of bifurcations has been found in large regions of the parameter space. As an example, we shall consider first the route to chaos for the system being on the lower branch at $\delta = 1.3\pi$, and $1.0 \leq \gamma\tau \leq 4.0$ (see Fig. 7).

The first Hopf bifurcation takes place at $\gamma\tau \approx 0.687\ldots$, a sequence of period-doublings starting from a period-1 solution and leading to quasi-periodicity at $\gamma\tau \approx 1.89$ joins. The quasi-periodic region ends at $\gamma\tau \approx 2.22$ with a period-2 solution which is doubled again for larger values of the delay-parameter.

At values of $\gamma\tau \geq 3.1$, the bifurcation diagram Fig. 7 shows a widening of the attractor. This behaviour extends to values $\gamma\tau > 4.0$. This sudden change in the size of a chaotic attractor is interpreted as a crisis, which is defined as a "collision between a chaotic attractor and a coexisting unstable fixed point or periodic orbit" [12].

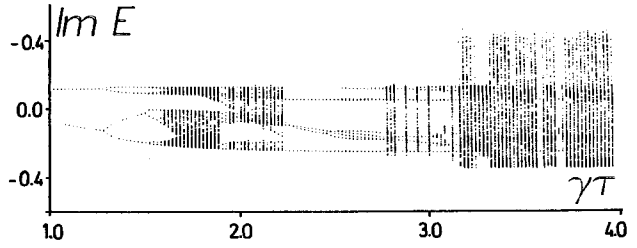

Fig. 7. Bifurcation diagram for the imaginary part of the electrical field $\mathrm{Im}\{E\}$ at $\delta = 1.3\pi$. Variation of the bifurcation parameter: $1.0 \leq \gamma\tau \leq 4.0$

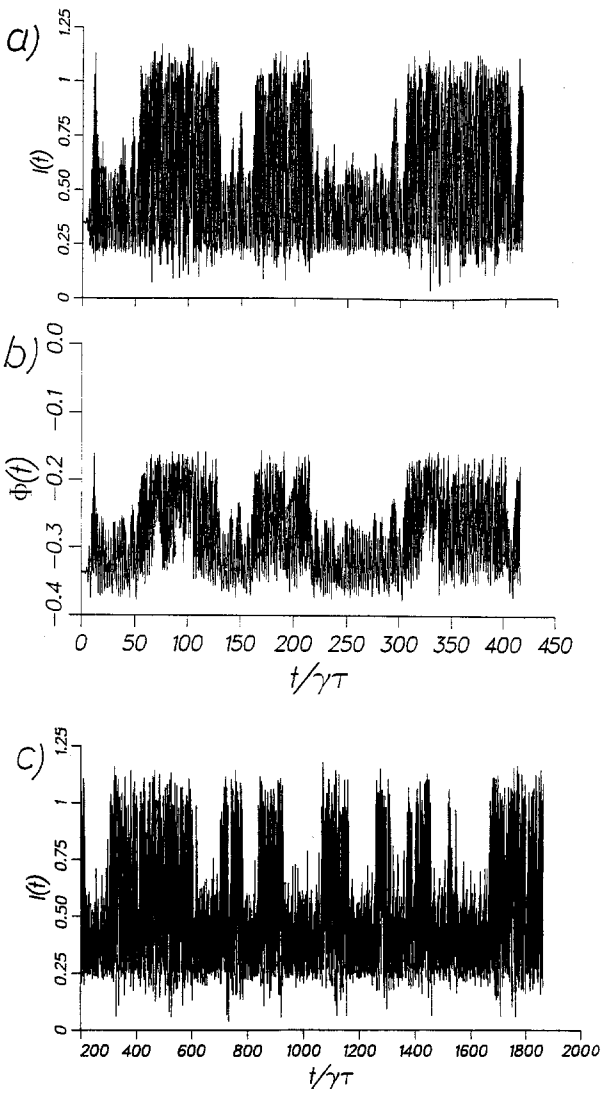

Fig. 8a-c. Intermittent time-series of the inversion and the transmitted intensity at $\delta = 1.3\pi$, $\gamma\tau = 4.0$. **a** Intensity and **b** Inversion, both for $t/\gamma\tau = 0$ to 425; **c** Intensity for $t/\gamma\tau = 200$ to 1900

A better understanding of the type of crisis is given by Figs. 8a,b. The time-series of the transmitted intensity of light and of the inversion is drawn. The figures were computed at parameter values $\delta = 1.3\pi$, $\gamma\tau = 4.0$ and with the initial conditions of the lower branch. One can see that the widening of the attractor is not transient but intermittent. The intermittent behaviour is a steady state solution (Fig. 8c).

The time-series of the inversion shows that the trajectory is in the domain of the middle branch when the transmitted light intensity is high and on the lower branch when the intensity is low. The position of the separating unstable fixed point between the two branches was found in a calculation for $\gamma\tau \to 0$ to be at $\Phi_u = -0.2535\ldots$.

The subsequent investigation shows that this crisis induced intermittency is an *intermittent bursting:* The first Hopf bifurcation on the middle branch takes place at $\gamma\tau = 0.1370\ldots$. While increasing $\gamma\tau$ the generated limit-cycle

expands in phase space and collides at $0.35 < \gamma\tau < 0.36$ with the separating saddle between the middle and the lower branch. Trajectories with initial conditions in the former basin of the middle branch now *fall* to the lower branch. This mechanism can be explained by the two-dimensional model of precipitation (see [6]).

In contrast to the middle branch, the trajectories of the periodic solution of the upper branch are limited to its basin of attraction. Therefore, a crossing of the boundary and a subsequent transition to other branches is not possible. The same behaviour holds for the other periodic, quasi-periodic and even chaotic solutions (see Fig. 7). Above $\gamma\tau \approx 3.1$ the chaotic attractor on the lower branch collides with the separatrix and extends to the saddle between middle and upper branch. In terminology of [13] we can call this behaviour *attractor widening*.

3 Conclusions

When investigating the behaviour of the ring cavity system on the lower branch a rich bifurcation structure is found. The period-doubling route is the main route to chaos in this system when the delay-parameter is varied. It is interrupted by a mode-locking region but continues afterwards. By variation of the other parameter (e.g., the input field E_i), we expect that similar bifurcation structures will be found.

At higher values of the delay-parameter the property of multistability becomes important: The coexistent solutions on the different branches tend to expand in phase space and the saddles between the branches cross. In great areas of the considered parameter space the phenomenon of precipitation occurs and we have distinguished three different cases.

- The solutions on different branches are periodic. In this case the two dimensional model of precipitation holds.
- Only one of the solutions involved is regular while the others are not. Here, the precipitation takes place in an at least three-dimensional phase space by the formation of a heteroclinic cycle.
- If the solutions on all of the involved branches are irregular the attractor widens in a crisis. The time-series shows intermittent bursts.

The transitions and jumps between different branches display very long transients. It takes many oscillations until the system can cross the *basin boundaries*, which are formed by regular or chaotic saddleorbits. The very complex behaviour in a three- or higher-dimensional phase space shows again that one has to consider the complete, infinite dimensional delay-differential equations if one wants to obtain the full dynamics of the multistable ring cavity.

Acknowledgements. The authors acknowledge gratefully useful discussions with M. Sauer. This study was partly supported by the Deutsche Forschungsgemeinschaft, Sonderforschungsbereich 185 'Nichtlineare Dynamik'.

References

1. K. Ikeda: Opt. Comm. **30**, 257–261 (1979)
2. M. LeBerre, E. Ressayre, A. Tallet, H.M. Gibbs: Phys. Rev. Lett. **56**, 274–277 (1986)
3. M. LeBerre, E. Ressayre, H.M. Gibbs, F.A. Kaplan, M.H. Rose: Phys. Rev. A **35**, 4020–4022 (1987)
4. B.J. Hawdon, J. O'Gorman, D.M. Heffermann: Z. Naturforsch. **46a**, 686–690 (1991)
5. D. Merkle, F. Kaiser: Phys. Lett. A **153**, 95–100 (1991)
6. F. Kaiser, D. Merkle: Phys. Lett A **139**, 33-140 (1989)
7. M. LeBerre, E. Ressayre, A. Tallet: Opt. Comm. **72**, 123–128 (1989)
8. M. Sauer, F. Kaiser: Appl. Phys. B **55**, 138–143 (1992)
9. R. Bonifacio, M. Gronchi, L.A. Lugiato: Opt. Comm. **30**, 129–133 (1979)
10. J. Guckenheimer, P. Holmes: *Nonlinear Oscillations, Dynamical Systems, and Bifurcations of Vector Fields* (Springer, New York 1983)
11. F.T. Arecchi, W. Gadomski, A. Lapucci, H. Mancini, R. Meucci, J.A. Roversi: J. Opt. Soc. Am. B **5**, 1153–1159 (1988)
12. C. Grebogi, E. Ott, J.A. Yorke: Physica D **7**, 181–200 (1983)
13. C. Grebogi, E. Ott, F. Romeiras, J.A. Yorke: Phys. Rev. A **36**, 5365-5380 (1987)